

# Silicon Micromechanics for the Fiber-Optic Information Highway

Cornel Marxer and Nico F. de Rooij

Institute of Microtechnology, University of Neuchâtel  
Jaquet-Droz 1, 2007 Neuchâtel, Switzerland

(Received June 29, 1998; accepted July 28, 1998)

**Key words:** electrostatic actuators, fiber-optic components, reflective modulator, fiber-optic switch, variable optical attenuator

Mechanical components such as switches, attenuators and filters are still widely used in today's fiber-optic networks despite the progress of integrated optics. Optomechanical devices offer several advantages with respect to their waveguide counterparts. Low insertion loss, low crosstalk, wavelength uniformity and polarization insensitivity are characteristics which are difficult to achieve with waveguides, whereas in devices using mechanical principles, several of the above performance requirements are readily obtained. Drawbacks of the existing bulk mechanical components, such as their large size, low speed and uncertain reliability can be overcome by using integrated micromechanics. Silicon micromechanics are reviewed for applications in future fiber-optic communication systems. We report on a reflective modulator for the access network, on a low-loss and low-crosstalk  $2 \times 2$  fiber-optic switch for network reconfiguration and protection, and finally on a four-channel variable attenuator for power equalization.

## 1. Introduction

The high-precision structuring techniques developed for integrated circuit industries can also be applied to build micromechanical structures. The first application of such small mechanical silicon parts in fiber-optic components was in alignment platforms to build small optical benches. Fiber alignment grooves have traditionally facilitated the attachment of fibers to photonic devices.<sup>(1)</sup> By preferential crystallographic wet etching<sup>(2)</sup> very precise V-shaped grooves can be formed in  $\langle 100 \rangle$  silicon and can be used for alignment. The accuracy of fiber alignment depends on the uniformity of the groove dimensions (0.2

$\mu\text{m}$  to  $1\ \mu\text{m}$ ) and the fiber geometry, i.e., its diameter and core concentricity. If the etching mask is well oriented to the crystal direction, reproducible alignment within a micrometer can be achieved with V-grooves. Several laser manufacturers use silicon motherboards for mechanical alignment and electrical and thermal interconnection<sup>(3)</sup> in their packaging. Additionally, silicon can be used as a base material for microlenses<sup>(3)</sup> and waveguides.<sup>(4)</sup>

In recent years it has been found that mechanical moveable structures and motors<sup>(5)</sup> can also be integrated into silicon using the same batch processing technology. Referred to as micro-electromechanical systems (MEMS), such structures can be used to build optical devices such as variable filters, switches and modulators. On reducing the size of a mechanical motor, its speed increases whereas the output force decreases. Optical devices are thus well-suited for miniaturization because no force is needed to redirect or modulate light. Optical MEMS can operate at a higher speed than their macromechanical counterparts, especially since the size of guided wave optics matches well with the dimensions used in MEMS. The on-chip microactuators can be integrated with the fiber alignment structures to allow a passively aligned assembly of the final system. This ability to build fast structures, self-aligned and already assembled on a silicon chip, is appropriate from a mechanical point of view, but there are also optical reasons which make optical MEMS an ideal candidate for high-performance fiber-optic components. Actually, in terms of insertion loss, crosstalk isolation, wavelength uniformity and polarization insensitivity, nothing can surpass a simple mirror. In particular, with respect to electrooptic or waveguide components, many unwanted effects can be avoided by applying mechanical principles.

In the present paper we will review three developments in the field of optical MEMS for application in future fiber-optic communication systems. The first component is a reflective duplexer for the access network. The second component is a highly reliable, low-loss  $2 \times 2$  switch for network reconfiguration and protection. The third component is a four-channel variable attenuator for power equalization in wavelength division multiplexed networks.

## **2. Modulator for Fiber-to-the-Home**

Today's full duplex, bidirectional single fiber-optic links operate with active light sources at both ends of the communication link. In contrast to conventional fiber-optic communication links with separate fibers for each direction, bidirectional links can be realized with only one fiber using the so called "BiDi" modules at both link terminals.<sup>(3)</sup> An alternative to this 'active-active' solution relies on reflective modulation, where part of the incoming light is used for the return channel. Several research groups have actively studied and demonstrated fiber-optic communication links based on reflective modulation.<sup>(6,7)</sup> During those investigations, it became clear that existing waveguide device technologies for reflective modulators suffer from two drawbacks. First, in comparison to active light sources, commercially available components are not competitively priced at present. This is mainly due to high processing and packaging costs. Furthermore, many devices suffer from polarization-dependent operating characteristics and comparatively high optical losses, factors which reduce the possible link length. The existing device types for

reflective modulators are based on electrooptic phenomena. In principle these effects provide extremely high modulation bandwidths beyond 40 Gbit/s.<sup>(8)</sup> However, in most practical cases high data transmission rates are only required in the 'downstream' direction from the service provider to the end user, whereas only a limited bandwidth is needed for transmission in the opposite 'upstream' direction. Modulation rates up to several Mbit/s can be achieved by using micromechanical modulators.<sup>(9-11)</sup> Based on silicon micromechanics, such modulators offer potentially low fabrication costs and can be produced in large quantities. Hence this technology can be more cost effective than an active-active link.<sup>(12)</sup>

Figure 1 shows the device architecture. The duplexer is composed of a single mode fiber carrying the in- and outgoing light, the micromechanical silicon modulator and the InGaAs photodiode chip for downstream data detection. The silicon chip forms the base plate, which carries the micromechanical modulator structure and the photodiode. The modulator is illuminated across the silicon substrate from a hole on the back. This hole reduces the distance between the fiber and the modulator in order to achieve a low insertion loss. Additionally the sidewalls of the hole passively align the single-mode fiber to the modulator on the top of the chip.

Figure 2 shows a scanning electron microscope (SEM) photograph of the micromechanical modulator. The two polysilicon electrodes form the mirrors of a Fabry-Perot cavity. When a voltage is applied between the two polysilicon layers, the free standing membrane is deformed by the electrostatic pressure and the optical path length between the mirrors is changed, resulting in modulation of the reflectivity. In Table 1 the overall characteristics are summarized and Fig. 3 shows a fully packaged component.

The modulator is inherently insensitive to polarization. The insertion loss is typically 1–3 dB. For a modulator with a bandwidth of 2–3 Mbit/s, a wavelength-dependent DC

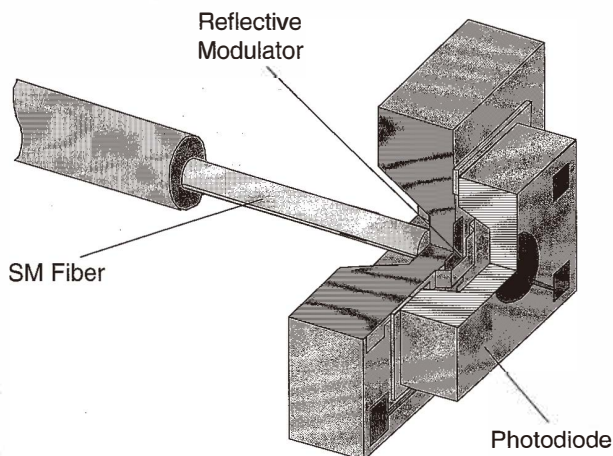


Fig. 1. Cross section of reflective duplexer.

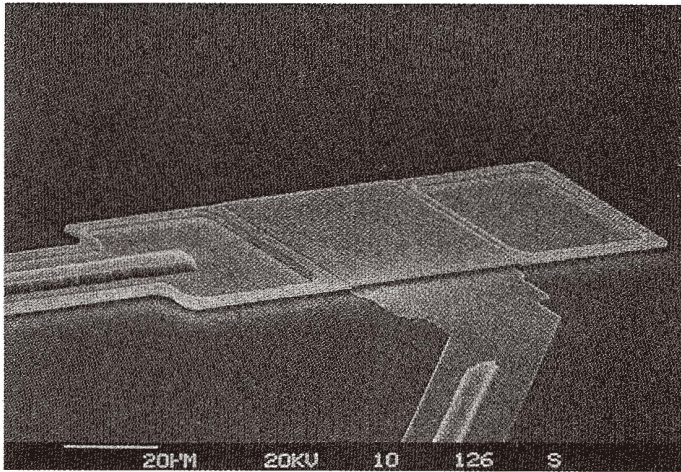


Fig. 2. SEM micrograph of Fabry-Perot modulator.

Table 1  
Measured modulator characteristics.

$\lambda$ [mm]	Insertion loss	On-off ratio	DC-bias	AC $V_{pp}$	Rise time
1260	< 3 dB	9 dB	90 V	5 V	< 200 ns
1310		10 dB	84 V	7 V	
1360		15 dB	69 V	17 V	

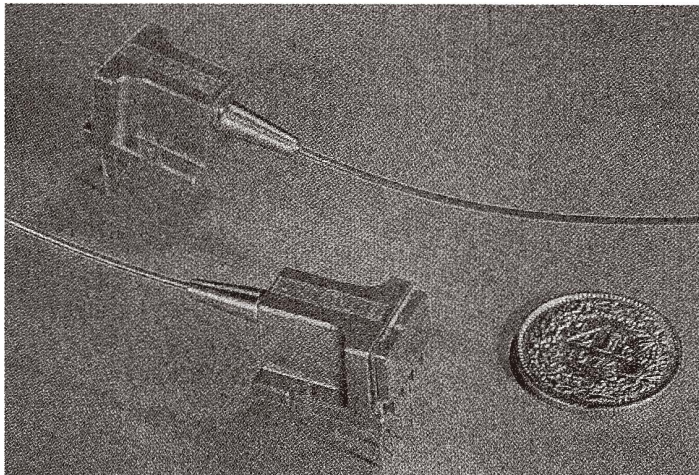


Fig. 3. Packaged reflective duplexer.

voltage of 69 – 90 V must be applied. A modulation voltage of 5 – 17 V is superimposed to achieve on-off ratios of typically 10 dB.

### 3. Fiber-optic $2 \times 2$ Switch

Switching of light from two input fibers to either of two output fibers is becoming increasingly important for allowing reconfiguration of fiber-optic networks down at the optical level. Also, for reasons of network security, there is a growing demand for highly reliable and stable switches. In order to recover quickly from a cable damage for example, the physical network layer must be reconfigured. In such an emergency a transparent optical switch can be used to rapidly reroute the data traffic around the network fault. Besides reliability, the switch should offer low insertion loss, low crosstalk and wavelength insensitivity. Currently, switches that meet these stringent requirements are based on bulk mechanics. They show excellent optical performance but are not sufficiently reliable for security applications. In addition, with a switching time of around 10 ms, they are rather slow.

On the other hand, there is a wide variety of fiber-optic switches based on effects in waveguides. Although these integrated fiber-optic switches are inherently fast, their high light loss and high crosstalk prevent a large-scale deployment. Consequently the mechanical switching principles offer the best optical performance for applications where speed is not critical.

In order to overcome some of the drawbacks of conventional mechanical switches, such as their large size, low speed, high cost and low reliability, the MEMS technology has been investigated for the fabrication of mechanical fiber optical switches. The mechanical switching principles are based on the movement of an optical element such as a prism, a diffractive optical element or simply a mirror. Figure 4 schematically shows a  $2 \times 2$  switch

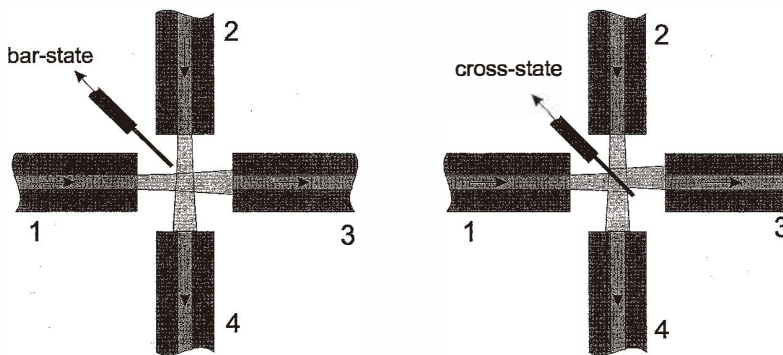


Fig. 4. Schematic top view of micromechanical  $2 \times 2$  switch. In the cross state the light travels straight. In the bar state the light beam is reflected at the vertical mirror. The thickness of the mirror introduces an offset of the beam between fibers 2 and 3.

using a micromirror. In the bar state, the light from the two pairs of fibers is coupled in a straight path between fibers No. 1 to No. 3 and between fibers No. 2 to No. 4. To switch into the cross state, the micromirror is brought into the optical path by linear displacement<sup>(13,14)</sup> or by 90° out-of-plane rotation<sup>(15)</sup> of the micromirror.

Similar designs of microfabricated switches, where the switching mirror was fabricated by polysilicon micromachining<sup>(13)</sup> or by the LIGA (a German acronym for Lithographie, Galvanoformung, Abformung) technique<sup>(14)</sup> have been proposed earlier. In our switch, the vertical mirror is fabricated by deep reactive ion etching (DRIE),<sup>(16)</sup> which allows the fabrication of the fiber grooves, the suspension structures and the actuator in the same etching step as the mirror. The mobile structures are released by sacrificial layer etching, i.e., by the time-stopped removal of a buried oxide of a silicon-on-insulator (SOI) wafer. The use of SOI wafers also allows a uniform etching depth to be obtained, i.e., the plasma etching stops when the buried oxide is reached. The height of the etched structures is 75  $\mu\text{m}$ , which is sufficient to cover the fiber core entirely when a single-mode fiber is placed into a groove of the same depth. To increase the reflectivity of the vertical mirror, the silicon is gold coated. In order to achieve a high crosstalk attenuation, this metal layer must be thick enough to prevent light from passing through the mirror. Figure 5 shows a SEM view of the plasma-etched vertical mirror in the center of the four alignment grooves and the electrostatic actuator.

Four fibers are placed into the alignment grooves at 90°. The cladding glass of the fiber is partially etched away in order to reduce the fiber diameter and to bring the fiber ends

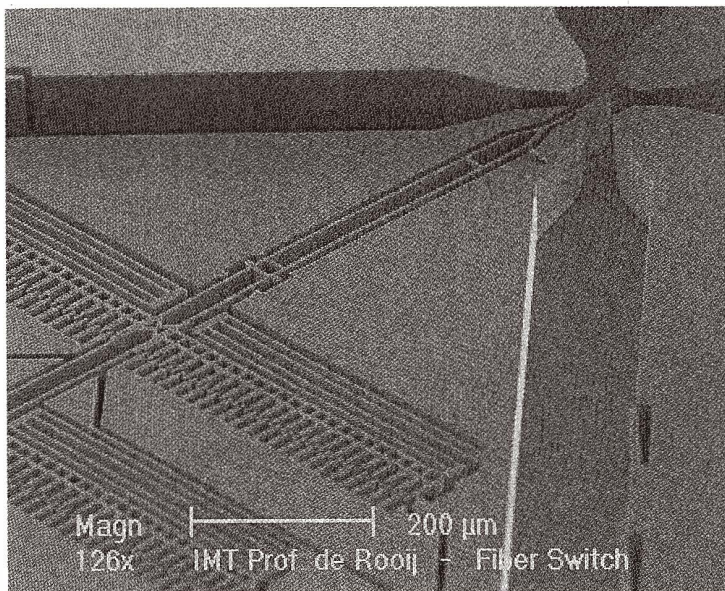


Fig. 5. SEM photograph of actuator-mirror structure of 2 × 2 switch.

closer together. The use of tapered fibers allows us to avoid any imaging optics. The light loss in the bar state is essentially limited to beam divergence. In the cross state, an additional loss arises due to the imperfection of the mirror. Additionally, as shown in Fig. 4, the mirror has a thickness which may introduce a lateral offset of the light beam, and this results in an additional loss in coupling between fibers No. 2 and No. 3. For a longitudinal offset of  $35\ \mu\text{m}$ , the theoretical light loss is below 0.3 dB for single-mode fibers in index-matching oil.

The switching mirror is actuated by an electrostatic comb drive actuator. When a voltage is applied between the two electrodes, an electrostatic force arises and pulls the mirror out of its rest position. When the voltage is reduced to zero, the mirror is pulled back again by the suspension springs. Since the moveable structure does not touch any other part, no sticking occurs. In addition, silicon is an excellent mechanical material, showing no fatigue in the absence of humid air.<sup>(17)</sup> This means that the micromechanical structure will function with high reliability and that the most current failure mode of micromechanism, i.e. sticking, is avoided by a design that does not include contacting surfaces. To switch the mirror out of the optical path, a displacement of over  $20\ \mu\text{m}$  is necessary. The electrostatic actuator delivers this displacement at a voltage of approximately 60 V. Figure 6 shows a fully packaged device, where the silicon chip is placed into a TO-8 package with a window for observing the mirror movement. A voltage converter circuit inside the package allows the electrostatic actuator to be driven with a 5 V supply voltage. The size of the entire package is only  $6 \times 3.5 \times 1.6\ \text{cm}^3$ .

For characterization, a switch was fully packaged and operated with its built-in voltage converter. To facilitate insertion loss measurements, the switch was connectorized. In the bar state, a minimum loss of 0.7 dB was measured. This value is close to the projected loss of 0.5 dB, where 0.3 dB would be from the longitudinal fiber gap and 0.2 dB from the

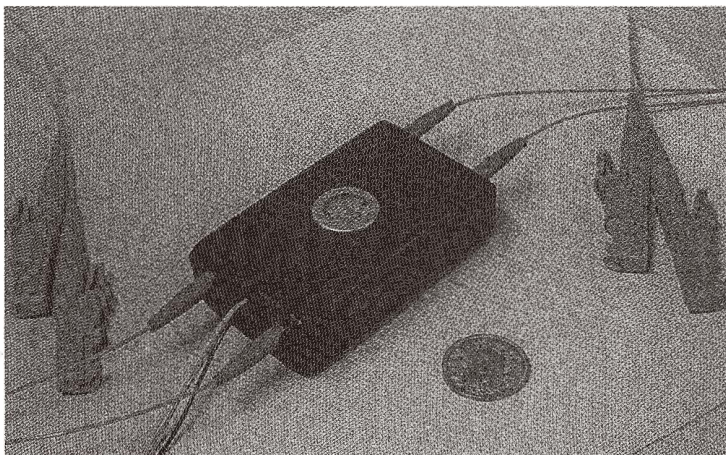


Fig. 6. Packaged fiber-optic switch with integrated driver electronics.

lateral offset of the fibers due to their eccentricity. In the cross state, the light is reflected on the vertical mirror and, as shown in Fig. 4, a lateral offset is introduced into one connection. Between fibers No. 1 and 4 the loss was 1.6 dB, whereas between fibers No. 2 and No. 3 the loss was 2.5 dB. This corresponds to a mirror reflectivity of 80% and a mirror thickness of about 1.6  $\mu\text{m}$ . The reflectivity of an ideally flat gold mirror would be over 97% at a wavelength of 1310 nm, the remaining 17% is lost through scattering due to the surface roughness.

The other optical characteristics of the switch also depend on the switching state. In the bar state, a crosstalk attenuation of over 60 dB was measured. The return loss was below -40 dB. In the cross state, i.e., when the light was reflected on the mirror, a small amount of light was still transmitted through the mirror and a crosstalk attenuation of 50 dB was measured. Also in the cross state, more light was returned back into the input fibers and a reflection loss of -33 dB was measured. This value can only be reduced by using a smoother mirror surface.

The oscilloscope trace in Fig. 7 shows a typical step response of the switch. The response time is around 0.5 ms, which is an order of magnitude faster than conventional mechanical switches. This notably higher speed is a direct benefit of the MEMS technology, which allows the fabrication of very small structures with lower inertia than that obtained using conventional techniques.

An overview of the switch performance is summarized in Table 2.

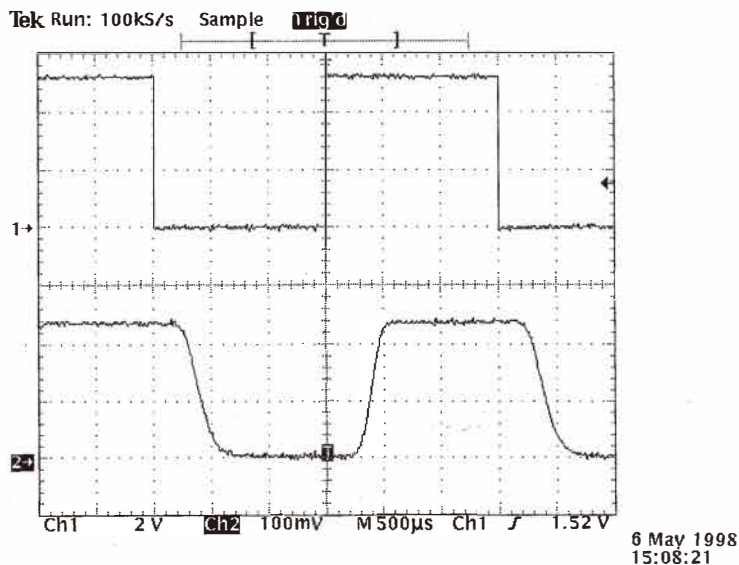


Fig. 7. Oscilloscope trace of switch response to a square wave of 330 Hz. Response time is 0.5 ms (time/div: 0.5 ms).

Table 2  
 Characteristics of MEMS-mirror-based switch (at 25°C).

	Bar state	Cross state
Insertion loss	0.7 dB	1.6 dB resp. 2.5 dB
Crosstalk attenuation	< -60 dB	< -50 dB
Backreflection attenuation	< -40 dB	< -33 dB
Switching speed	< 1 ms	
Driving voltage	5 V CMOS	
Supply voltage (power)	5 V (70 mW)	

#### 4. Variable Attenuator

A particular advantage of micromachining technology is that many identical devices can be fabricated in parallel not only on a wafer but also on an individual chip. An application where it is particularly interesting to execute the same function independently on several fibers is power tuning in wavelength division multiplexing (WDM) networks. In this network architecture, the information is carried on several wavelengths transmitted through a single optical fiber. The capacity of the link can be increased by adding surplus wavelengths into the fiber. For long-distance transmission, all the wavelengths are amplified in parallel in erbium-doped fiber amplifiers. With such optical amplifiers, the electro-to-optical conversion required in the conventional repeaters becomes unnecessary. Nevertheless, all optical wavelengths should be at the same optical power to allow proper functioning of the amplifier. In particular, at the output of an add/drop module or an optical cross-connect, the power level of each wavelength depends on the current configuration of the network and might change with every reconfiguration. To avoid error in transmission, the power level at each wavelength must be adjusted by a variable attenuator.<sup>(18)</sup>

Conventional variable attenuators are optomechanical. They operate by stepwise movement of a shutter into the expanded optical beam between an input and an output fiber. Depending on the position of the shutter, more or less optical power is coupled to the output. As schematically shown in Fig. 8, the use of micromechanics allows us to avoid any imaging optics, because the fiber ends can be brought sufficiently close together. Additionally, the smaller shutter has a faster response time.

As with the 2 × 2 switch, the micromechanical attenuator is fabricated using the same technology, which allows the integration of the shutter with its electrostatic actuator and the fiber alignment grooves. Figure 9 shows a SEM micrograph of the obtained structure, where three of the four parallel attenuators can be seen. The middle shutter is closed, whereas the outer two actuators are in a rest position. The shutters are at an 82° angle with respect to the fiber channels. Light reflected from the mirror is at 16° to the fibers and is no more guided. This allows a very low return loss to be achieved.

Figure 10 shows a packaged four-channel variable attenuator. The insertion loss is around 1.5 dB. When the voltage on the electrostatic actuator is increased, the vertical shutter is moved into the optical path between the input and the output fiber, resulting in

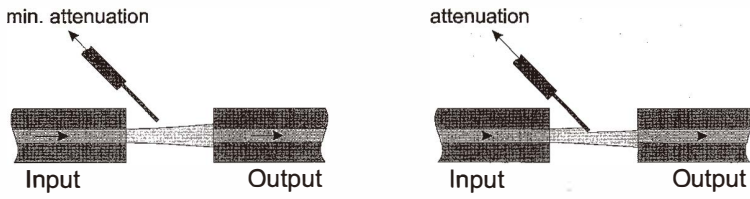


Fig. 8. Schematic top view of micromechanical variable attenuator.

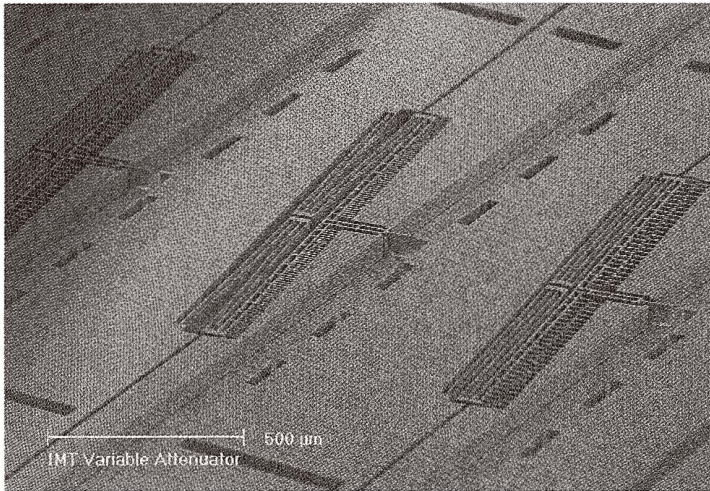


Fig. 9. SEM micrograph of actuator-shutter structure of three variable attenuators.

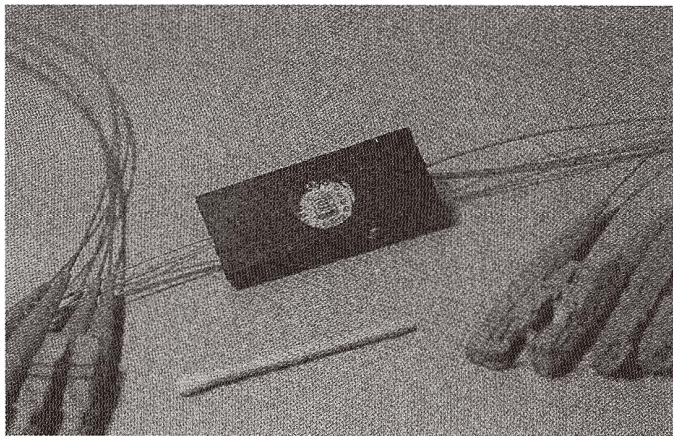


Fig. 10. Packaged four-channel variable attenuator.

coupling attenuation. Figure 11 shows the static voltage attenuation behavior. During the application of the first 20 V the attenuation is practically unchanged, because the shutter is still out of the optical path. Increasing the voltage results in a smooth increase in the attenuation at a rate of about 1 dB/V. Above 10 dB attenuation, this rate increases rapidly but stays continuous. The response of the attenuator is not linear but increases monotonically. Using a feedback control loop and a voltage converter, operation with a 5 V analog voltage is feasible. At a voltage of 43 V, a maximum attenuation of over 50 dB can be obtained. The reflection loss was measured to be above 37 dB. These results are summarized in Table 3.

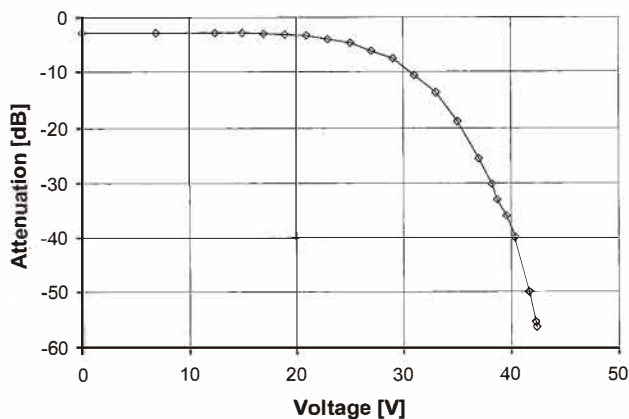


Fig. 11. Static response of attenuation versus voltage.

Table 3  
Characteristics of four-channel variable attenuator.

Insertion loss	1–3 dB
Maximum attenuation	< – 55 dB
Reflection loss	< – 37 dB
Maximum voltage	44 V

## 5. Conclusions

We have reported on three MEMS-based components for fiber-optic communications. All devices take advantage of the silicon micromachining technology not only for their functionality but also to allow self-aligned positioning of the single-mode fibers. Therefore they have the potential for low fabrication cost and mass production.

### Acknowledgments

The authors would like to acknowledge the valuable support from Patrick Griss. Parts of this work were funded by the Swiss priority program MINAST, by Ascom Tech Ltd., Berne, and by the TMR network of the European Community.

### References

- 1 E. J. Murphy and T. C. Rice: IEEE Journal of Quantum Electronics **QE22 No. 6** (1986) 928.
- 2 D. B. Lee: J. Appl. Phys. **40** (1969) 4569.
- 3 H. L. Althaus, W. Gramann and K. Panzer: Proceedings of 47<sup>th</sup> Electronic Components and Technology Conference, May 18–21, San Jose, Ca, (1997) p. 7.
- 4 C. K. Tang *et al.*: J. Lightwave Tech. **12** (1994) 1394.
- 5 C. Linder, L. Paratte, M. -A. Gretillat, V. P. Jaecklin and N. F. de Rooij: J. Micromech. Microeng. **2** (1992) 122.
- 6 L. Altwegg, A. Azizi, P. Vogel, Y. Wang and F. Wyler: J. Light. Tech. **12** (1994) 535.
- 7 P. J. Duthie, M. J. Wale, I. Bennion and Hankey: Electron. Lett. **22** (1986) 517.
- 8 R. G. Walker: J. Light. Tech. **LT-5 No. 10** (1987) 1444.
- 9 C. Marxer, M. A. Gretillat, V. P. Jaecklin, R. Baettig, O. Anthamatten, P. Vogel and N. F. de Rooij: Sensors and Actuators A **52** (1996) 46.
- 10 J. A. Walker, K. W. Goosen and S. C. Arney: J. of Micro-Electromechanical Systems, **5 No. 1** (1996) 45.
- 11 O. Anthamatten, R. Bättig, B. Valk, P. Vogel, C. Marxer, M. A. Gretillat, N. de Rooij: Digest of IEEE/LEOS 1996 Summer Topical Meeting, Optical MEMS and their Applications, Keystone Co, USA (1996) p. 61.
- 12 N. J. Frigo, P. P. Iannone, P. D. Magill, T. E. Darcie, M. M. Downs, B. N. Desai, U. Koren, T. L. Koch, C. Dragone, H. M. Presby and G. E. Bodeep: IEEE Photonics Technology Letters **6 No. 11** (1994).
- 13 S. S. Lee, L. Y. Lin and M. C. Wu: Elec. Lett. **31** (17) (1995) 1481.
- 14 J. Mohr, M. Koh and W. Menz: 7<sup>th</sup> Int. Conf. on Solid-State Sensors and Actuators (Transducers '93), Jun. 7–10, (1993) p. 120.
- 15 H. Toshiyoshi and H. Fujita: Tech. Dig. 8<sup>th</sup> International Conference on Solid-State Sensors and Actuators (Transducers '95), Stockholm, Sweden, **1** (1995) p. 297.
- 16 C. Marxer, C. Thio, M.-A. Gretillat, O. Anthamatten, R. Baettig, B. Valk, P. Vogel and N. F. de Rooij: IEEE J. of Micro-Electromechanical Systems **6 No. 3** (1997) 277.
- 17 C. Marxer, M. A. Grétilat, R. Baettig, O. Anthamatten, P. Vogel and N. F. de Rooij: Sensors and Actuators A **61** (1997) 449.
- 18 J. E. Ford, J. A. Walker and K. W. Goosen: Conference on Microelectronic Structures and MEMS for Optical Processing, 29–30 Sept. 1997, Austin, Texas, **Spie Vol. 3226** (1997) p. 86.